Metrol. Meas. Syst., Vol. 28 (2021), No. 4
DOI: 10.24425/mms.2021.137700

PAN POLSKA AKADEMIA NAUK

METROLOGY AND MEASUREMENT SYSTEMS

Index 330930, ISSN 0860-8229
www.metrology.wat.edu.pl

M&MS

COMPARISON OF MULTIBAND FILTERING, EMPIRICAL MODE DECOMPOSITION AND SHORT-TIME FOURIER TRANSFORM USED TO EXTRACT PHYSIOLOGICAL COMPONENTS FROM LONG-TERM HEART RATE VARIABILITY

Krzysztof Adamczyk, Adam G. Polak

Department of Electronic and Photonic Metrology, Wrocław University of Science and Technology, B. Prusa Str. 53/55, 50-317 Wrocław, Poland (✉ *krzysztof.adamczyk@pwr.edu.pl, adam.polak@pwr.edu.pl*)

Abstract

Heart rate is constantly changing under the influence of many control signals, as manifested by heart rate variability (HRV). HRV is a nonstationary, irregularly sampled signal, the spectrum of which reveals distinct bands of high, low, very low and ultra-low frequencies (HF, LF, VLF, ULF). VLF and ULF components are the least understood, and their analysis requires HRV records lasting many hours. Moreover, there are still no well-established methods for the reliable extraction of these components. The aim of this work was to select, implement and compare methods that can solve this problem. The performance of multiband filtering (MBF), empirical mode decomposition and the short-time Fourier transform was tested, using synthetic HRV as the ground truth for methods evaluation as well as real data of three patients selected from 25 polysomnographic records with clear HF component in their spectrograms. The study provided new insights into the components of long-term HRV, including the character of its amplitude and frequency modulation obtained with the Hilbert transform. In addition, the reliability of the extracted HF, LF, VLF and ULF waveforms was demonstrated, and MBF turned out to be the most accurate method, though the signal is strongly nonstationary. The possibility of isolating such waveforms is of great importance both in physiology and pathophysiology, as well as in the automation of medical diagnostics based on HRV.

Keywords: heart rate variability, nonstationary signal analysis, multiband filtering, empirical mode decomposition, short-time Fourier transform, Hilbert transform.

1. Introduction

Heart rate (HR) is constantly changing under the influence of many internal signals. *Heart rate variability* (HRV), resulting from decelerations and accelerations in the HR [1], is traditionally determined by founding the RR intervals from the QRS complexes of the *electrocardiographic* (ECG) signal, however, alternative methods for analysing cardiac activity are also being developed [2]. The *autonomic nervous system* (ANS) controls the HR through the activity of the *sympathetic* (SNS) and the *parasympathetic nervous system* (PNS). Increased SNS activity or decreased PNS activity causes an increase in the HR and vice versa [3], however their relationship is quite complex [4].

When analysing the HRV spectrum, it is possible to distinguish frequency bands with factors that affect them. The *high frequency* (HF) band (0.15-0.4 Hz) mainly reflects the activity of the PNS with the vagus nerve. It is also synchronised with the respiratory cycle (respiratory sinus arrhythmia), which causes the HR to accelerate during inhalation and slows it down during

Article history: received March 21, 2021; revised June 18, 2021; accepted June 23, 2021; available online July 5, 2021.

exhalation. Respiration affects cardiovascular parameters not only through the ANS but also through mechanical paths [4-8]. The *low frequency* (LF) band (0.04-0.15 Hz) is affected primarily by *blood pressure* (BP) through the baroreflex system and both PNS and SNS. During rest, the LF band reflects baroreflex activity without the SNS [4-8]. The *very low frequency* (VLF) band (0.004-0.04 Hz) is not known well enough to precisely define factors affecting it. They may include physical activity [9], thermoregulation [10, 11] renin-angiotensin [12] and humoral factors [13], as well as the intrinsic nervous system [4]. The *ultra-low frequency* (ULF) band (<0.004 Hz) is all the more not well understood. The effect of the circadian rhythm on ULF is most commonly suggested [7, 8, 14]. Other potential factors may include core body temperature, metabolism and the renin-angiotensin system. There is no consensus on the contribution of PNS and SNS to the ULF component [4]. In conclusion, there are no clearly identified factors influencing VLF and ULF, and quantitative information is lacking in all cases. The only exception is the well-known relationship between the respiratory rhythm and HF. The above premises emphasize both the significance of information inherent in the traces of these four components as well as the importance of methods for their extraction and deeper analysis.

HRV frequency analysis can be performed on short or long signal fragments. The short-term analysis usually includes fragments of 5 minutes or less. This approach allows minimising the impact of signal non-stationarity [15, 16]. However, such an analysis is not suitable for extracting the lowest frequencies of the ULF band. Long-term analysis (*e.g.* 24 hours) shows the ULF [7], but then the stationarity problem is much more serious [17]. Outliers in the HRV signal can be modified, but in the case of short-term analysis, often unrepresentative fragments are simply discarded entirety [18-20]. Yet another approach is online analysis [21, 22], which, by definition, shares many features with the short-term one. HRV is an irregularly time-sampled signal and many research has followed the suggestion to work with an evenly spaced signal after interpolation [17]. The most common method is cubic spline interpolation, often with 4 Hz sampling rate in case of humans [16, 22-25].

Most often, frequency analysis is performed using the *fast Fourier transform algorithm* (FFT) or autoregressive modelling, which requires to find an optimal model order [25, 26]. Other methods include higher-order moment spectra and cumulants of a signal [3] or *short-time Fourier transform* (STFT) used to determine the local frequency components of quasi-stationary signal fragments [3, 22, 25]. An alternative to STFT for studying the nonstationary signals is the continuous wavelet transform returning the correlation coefficients between the signal and the rescaled wavelet of finite length and energy [3, 25]. Another popular method is the *empirical mode decomposition* (EMD), which extracts oscillating components with symmetric envelopes (called the *intrinsic mode functions*, IMFs) from a nonlinear and nonstationary signal and is suitable for the further determination of instantaneous amplitudes and frequencies with the use of the Hilbert transform (collectively called the *Hilbert-Huang transform*, HHT) [27]. It was used, among others, to study the information transaction among the IMFs [28] or to identify the HRV component associated with breathing [29]. Likewise, EMD was applied to analyse the HF component of foetal HRV reconstructed from IMFs with frequency content higher than 0.3 Hz [30]. Foetal HRV was also investigated in [25], where the sum of the last IMFs was used as a surrogate of the VLF component. Echeverria et al. applied HHT to derive IMFs from 5 min long series gathered from the PhysioNet database. In this way they succeeded in showing the frequency content of the IMFs, which, however, overlapped in the range of VLF to HF [23]. Similarly, EMD was used to investigate changes in the HRV spectrum after atropine administration [31]. Neto *et al.* proposed to enhance the analyses of IFMs by successively adding them from the coarse to fine and from fine to coarse ones [32]. In the work by Ihlen *et al.*, the authors concluded that instantaneous frequencies and amplitudes estimated for HF and LF components from normal sinus arrhythmia should be interpreted with caution because of the mode mixing which produced artificial fluctuations [33]. Similar

observations were reported in [16]. Another interesting attempt was the use of EMD to online analysis of HRV by the extrapolation of IMFs related to LF and HF, to determine instantaneous frequencies and powers, with delays reduced to 60% compared to the STFT [22].

The above-mentioned applications of EMD for HRV frequency analyses demonstrate also a potential usefulness of other time-domain methods for signal decomposition when combined with HT. In the 1980s, *multiband filtering* (MBF) was popular in partitioning HRV within specific frequency bands [24], however later this approach was generally abandoned in favour of nonlinear methods, better suited to nonstationary signals, including adaptive filters operating on irregularly sampled data [34,35]. Since then, MBF or high-pass filters have usually been applied to correct the HF spectrum [25, 29, 36, 37], though they showed no significant difference in comparison with the adaptive nonlinear filters [36]. Nevertheless, MBF was recently used to separate the original HRV waveform into the higher frequency bands [28,38].

The above survey of related research reveals that the problem of reliable extraction of the well-recognised frequency components from overnight HRV remains unsolved. Many studies analysed the HRV spectrum, in particular by determining its power in certain ranges using FFT or autoregressive modelling [39]. In addition, the HF range was often investigated due to its connection to the respiratory signal, but lower frequencies were not so popular, in particular ULF. On the other hand, knowledge of the actual waveforms of the HF, LF, VLF and ULF components is vital in better identification and analysis of the function of various physiological systems and couplings between them. Therefore, the work is aimed at analysing the effectiveness of methods with the potential to extract physiological components (especially of low and ultra-low frequencies) from long-term HRV to finally identify the most accurate approach to this highly nonstationary signal processing. Based on the literature to date, it was decided to test the performance of MBF, EMD and STFT first. The main hypotheses underlying this work are that HRV represents a non-uniformly sampled sum of the effects of distinct physiological drives regulating HR that can be separated in the frequency domain, and these effects are taken as components of hypothetical *continuous heart rate variability* (cHRV).

In the following, the data used and applied methodology are described, the results obtained are presented and discussed, and finally the main conclusion is drawn about the best method among the tested ones.

2. Material and Methods

All simulations and calculations were made in MATLAB R2020a (The MathWorks, USA) using its standard functions with default parameters (unless stated otherwise) on a PC (Windows 10, Intel Core i3-4130, CPU@3.40 GHz, RAM 8 GB).

2.1. Physiological data

The data come from the St. Vincent's University Hospital Sleep Disorders Clinic in Dublin available from the PhysioNet database [40]. There are many other databases on the PhysioNet platform, but patients were either physically active or were influenced by changing conditions or medications. What was needed was a database of ECG records and breathing signals in neutral state, lasting many hours. Polysomnographic studies [41] meet the criteria and in addition, potential sleep apnea extends the range of HF values related to respiration. The chosen database contains 25 overnight polysomnographic recordings of patients with no known cardiac disease, autonomic dysfunction, and no medication affecting heart rate. ECG sampled at 128 Hz and the respiratory signal sampled at 8 Hz were used in this study.

These ECG recordings were used to derive HRV signals (next subsection), and then HRV spectrograms were computed for each subject using the STFT. The spectrograms were

compared by visual inspection and three of them (from Patients #5, 7 and 11), with the most visible trace of HF, were selected for further processing. The criterion of a good quality HF traces is important due to the subsequent comparisons of the HF components extracted from HRV with recorded respiration, as these are directly correlated signals. In addition, the first 54 min of Patient #11 data were removed due to visible effects of electrode disconnection.

2.2. Data preprocessing

The ECG was upsampled ten times (nonlinear interpolation) to 1280 Hz to get a higher resolution of R peaks in time, and thus to more accurately define the RR intervals. PhysioToolkit software package was used to find the QRS complex [40] and the exact location of the R peak was determined as the signal maximum near this region. The RR signal was created as the difference in time between consecutive R peaks.

It is common that the ECG (and thus HRV) signal is disrupted by artefacts of various origins, and the effects of some of them may be seen as extreme values [42]. Many methods for HRV artefacts removal have been proposed, but in this work special attention was paid to keeping the timeline unchanged, otherwise the component phases would be distorted in the rest of the signal. For this reason, any extreme value representing instantaneous HR above 98 bpm (RR < 0.61 s) was added to its larger neighbour, creating a new surrogate RR. On the contrary, when HR was lower than 49 bpm (RR > 1.22 s), the corresponding RR was split into two equal surrogates. These limits of 49-98 bpm were adopted taking into account sleep conditions. Although the above procedure modified the outliers of HRV, it only happened locally, preserving all other data and the original timeline.

Giving this restored HRV, the timeline was reconstructed as a cumulative sum of its values (RR intervals). Then cubic splines were applied to interpolate the non-uniformly sampled HRV at 10 Hz. After using an antialiasing zero-phase filter (0.5 Hz cut-off frequency), the signal was finally resampled to 2 Hz, and is hereinafter referred to as HRV_2.

The respiratory signal (Resp) was preprocessed in a similar way. First, it was bandpass filtered in the range of 0.15-0.40 Hz, and then resampled to 2 Hz for comparisons with the HF component of HRV_2.

2.3. Multiband filtering

The first of analysed methods was classical *multiband filtering* (MBF). It allows to preserve the frequency content of a signal in a given passband while attenuating all others and can be used only when the lower and upper cut-off frequency are defined. Therefore the frequency ranges of searched components, hereinafter referred to as: HFc (0.15-0.40 Hz), LFc (0.04-0.15 Hz), VLFc (0.004-0.04 Hz), and ULFc (0-0.004 Hz) were used. The digital passband, zero-phase (not distorting the shapes of the extracted components), minimum-order, finite impulse response (FIR) filters were designed to have a stopband attenuation of 60 dB. Their outputs are convolutions of filter coefficients and last signal samples, the number of which is called the filter order. These filters were used to extract the three higher frequency components, and an analogous lowpass one (only with the upper cut-off frequency) for the ULFc.

2.4. Empirical mode decomposition

Empirical mode decomposition (EMD) is a method dedicated for the analysis of nonstationary signals. It allows to automatically extract a finite number of oscillating components called the *intrinsic mode functions* (IMF) without any a priori assumptions. The IMFs are characterised by the number of extrema the same as the number of zero crossings and

symmetrical envelopes in relation to the zero line. The EMD recurrent procedure, first proposed in [27], was also extensively described in [23, 28, 29, 32]. After decomposition, the signal can be represented as a sum of IMFs denoted here as $x_c(t)$ and the final residue $r_p(t)$:

$$x(t) = \sum_{c=1}^{p} x_c(t) + r_p(t) . \tag{1}$$

The number of IMFs as well as their frequency contents are not known in advance, depending only on the nature of the analysed signal, in particular, several IMFs may represent a given physiological component. Therefore, the maximal number of extracted IMFs was set at 16, and for each of them, the instantaneous frequencies were calculated (Subsection 2.6) and an empirical histogram was generated from their values. A given IMF was labelled as representing one of the searched components based on the maximum number of counts that fall within the specified frequency range on the histogram. Then all IMFs with the same label were summed to obtain the corresponding HFc, LFc, VLFc and ULFc. The residue, representing the slowest variations, was finally added to the initial ULFc.

2.5. Short-time Fourier transform

One of the most popular methods for frequency analysis of nonstationary signals is the *short-time Fourier transform* (STFT), assuming signal local stationarity inside a short-time moving window. At each window position, the FFT is calculated from its samples (the result is often converted to power density and presented in dB), giving a local spectrum associated with a specific time coordinate. This discrete spectrum is, unfortunately, only an estimate of the real one due to windowing (resulting in spectrum leakage and scalloping) and it changes with the position of the window. A set of such spectra, arranged one after another, with the power density shown on a colour scale, form together a time-frequency graph called the spectrogram.

Since the searched components have defined, but different frequency contents, the widths of the analysing windows were selected as equal to the period of the lowest frequency in the corresponding range of HF, LF and VLF, *i.e.* 6.5, 25 and 250 s respectively. For ULF it was arbitrary set to 30 min. The windows were shifted by 1 sample of HRV_2 and the results of computations were assigned to time coordinates corresponding to their centres.

The analysis took several steps. After the mean removal, the Hann window was applied, then the signal was zero-padded to 2000 samples (giving a frequency resolution of 1 mHz) and the FFT was computed. Having a complex spectrum $X(f)$, the spectral energy density $E(f)$ for each frequency was computed taking into account the squared amplitude $E = A^2 = |X|^2$, lengths of signal and Hann window, and the coefficient of energy loss caused by windowing. Finally, the instantaneous amplitude was assessed as:

$$A_c(t) = \sqrt{\sum_{f=f_{lo}}^{f_{hi}} E(f)} , \tag{2}$$

where t is the coordinate of the window centre, and f_{lo} and f_{hi} denote the limits of the given frequency range. Analogously, the instantaneous phases were calculated as the angles of $X(f)$, and then their average value $\varphi_c(t)$ in the given frequency range. The instantaneous magnitudes of searched components were synthetized as:

$$x_c(t) = A_c(t) \sin\left(\varphi_c(t)\right) . \tag{3}$$

In addition, the instantaneous mean from the ULF analysis was added to the initial ULFc. Finally, all the extracted components were passband or lowpass filtered using the filters designed for the MBF method.

2.6. Instantaneous amplitudes and frequencies

As the nonstationary HRV components and Resp signals are supposed to be *amplitude* (AM) and *frequency modulated* (FM), the instantaneous amplitudes (envelopes) and frequencies are of great interest. They can be derived using the *Hilbert transform* (HT).

The applied HT returned analytic signals X_c from the real components x_c:

$$X_c(t) = x_c(t) + jh_c(t) = A_c(t)e^{j\varphi_c(t)}, \tag{4}$$

where h_c is the HT of x_c. The analytic signals clearly determined A_c and φ_c, and then the instantaneous frequencies of components f_c were calculated after φ_c unwrapping:

$$f_c(t) = \frac{1}{2\pi}\frac{d\varphi_c}{dt}. \tag{5}$$

2.7. Signal postprocessing

One of the well-known problems with HT use are the emerging negative frequencies [43]. They result from numerical differentiation of instantaneous phases which are not sufficiently smooth. To deal with this effect, all frequency samples outside the range of analysed component were discarded and the rest smoothed with a median filter of the same order as the relevant window size. The instantaneous amplitudes were also smoothed in the same way.

2.8. Generation of synthetic HRV

Ground truth is necessary to compare and quantify the proposed methods, but it cannot be deduced for real HRV data, therefore synthetic signals are used to this end [16, 22, 23, 25, 31, 33]. In this work, a synthetic 6-hour HRV series was generated, consisting of nonstationary HF, LF, VLF and ULF components. All the components were simulated as AM and FM signals. This means that both the component amplitudes and frequencies had their own ranges of magnitude variation represented by A_{am0}, A_{am} and A_{fm0}, A_{fm} respectively, and modulation frequencies f_{am} and f_{fm}:

$$\begin{aligned} A_c(t) &= A_{am0} + A_{am}\sin\left(2\pi f_{am}t\right), \\ \varphi_c(t) &= 2\pi A_{fm0}t + A_{fm}/f_{fm}\sin\left(2\pi f_{fm}t\right). \end{aligned} \tag{6}$$

These parameters were assessed from the analyses of Patient #5, 7 and 11 data (Subsection 3.3, Table 1). Then (3) was applied to compute the synthetic components that were finally summed together and further shifted up by a constant of 0.95 s, forming the continuous cHRV sampled at 1 kHz [17]. Next, taking into account the relationship between HRV values and the timeline (every new value HRV(t_i) lies on cHRV and is equal to RR(t_i) = $t_i - t_{i-1}$), the irregularly spread HRV samples were found. Finally, HRV was made more realistic by adding Gaussian noise [25], with the standard deviation of 0.01 s.

Metrol. Meas. Syst., Vol. 28 (2021), No. 4
DOI: 10.24425/mms.2021.137700

2.9. Evaluation of methods accuracy

The effectiveness of the analysed methods could be evaluated in two ways. Firstly, the HF components extracted from the real HRV were compared with the simultaneously recorded Resp signal, and secondly, all the components extracted from simulated HRV were compared to their synthetic counterparts (ground truth). In the former case, both signals were standardised before matching them due to their different magnitudes. In the latter one, two measures of similarity were calculated: the relative error of extraction:

$$\delta_{ex} = \frac{\|x_c - x_s\|_2}{\|x_s\|_2} 100\% , \tag{7}$$

where $\|\bullet\|_2$ stands for the Euclidean norm, x_s is for a synthetic and x_c for an extracted component, as well as the Pearson correlation coefficient r between corresponding samples.

3. Results

3.1. Validation of HRV simulation and reconstruction

The primary question in extracting the continuous components from irregularly spread data is the quality of the relationship between reconstructed, regularly resampled HRV_2 and the underlying cHRV, as well as whether the simulated cHRV covers the main properties of real HRVs. To this end, power spectral densities (PSD, Welch method, Hann window of 60 samples, zero-padding to 2000 samples, 90% overlapping) of real HRVs were compared with that of cHRV (Fig. 1a), and the HRV_2 samples obtained from the simulated undistorted and distorted HRVs were plotted against the cHRV (Fig. 1b). The obtained results show that the PSD of the synthetic signal (black curve) matches the real PSDs well. Also it is visible that the resampled HRV_2 with the timeline restored from undistorted HRV (red dots) perfectly fits cHRV. Otherwise it is with the samples of HRV_2 restored from distorted HRV, which show the effect of additive random disturbances, preserving however the main course of cHRV.

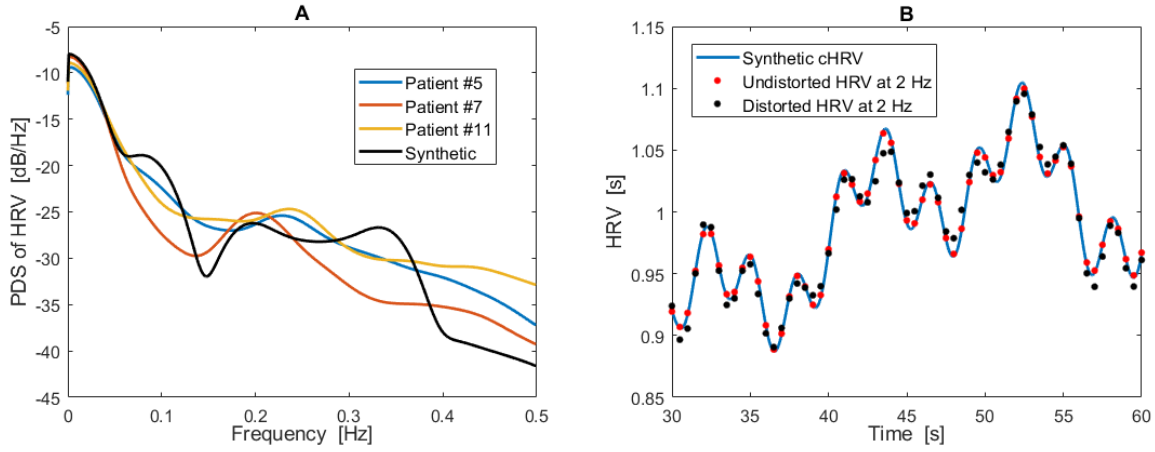

Fig. 1. A) Power spectral densities of HRVs from three patients and synthetic distorted data; B) synthetic undistorted and distorted HRVs resampled to 2 Hz plotted against the underlying continuous cHRV.

3.2. HF, LF, VLF and ULF components

The traces of frequency components extracted from HRVs of Patient #5, #7 and #11 using the three proposed methods are shown in Figs 2-3. To the best of our knowledge, such an overnight nature of physiological drives has not yet been demonstrated, especially in the case of VLF and ULF. The main observation is that the methods yielded virtually very similar patterns of the components for a given patient, proving both their usefulness in solving the problem, as well as the reliability of the extracted waveforms.

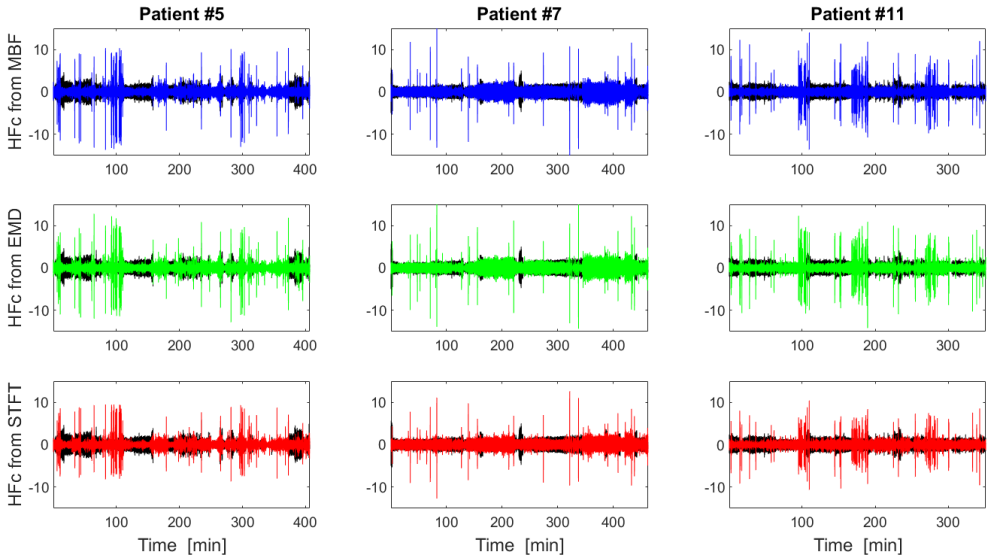

Fig. 2. Standardised high frequency components (HFc) extracted from HRVs of three patients using the three proposed methods: MBF (blue), EMD (green) and STFT (red) shown against the standardised respiratory signals (black).

On the other hand, matching among respiratory waveforms and HFc magnitudes is weak (Fig. 2), which draws more attention to the known frequency coupling between these two signals. The phases extracted from the corresponding Resp and HFc signals showed good consistency and high correlation between their samples (r = 0.84, 0.93 and 0.93 for MBF and Patient #5, 7 and 11, respectively), confirming the high compatibility of phases characterising both two sources.

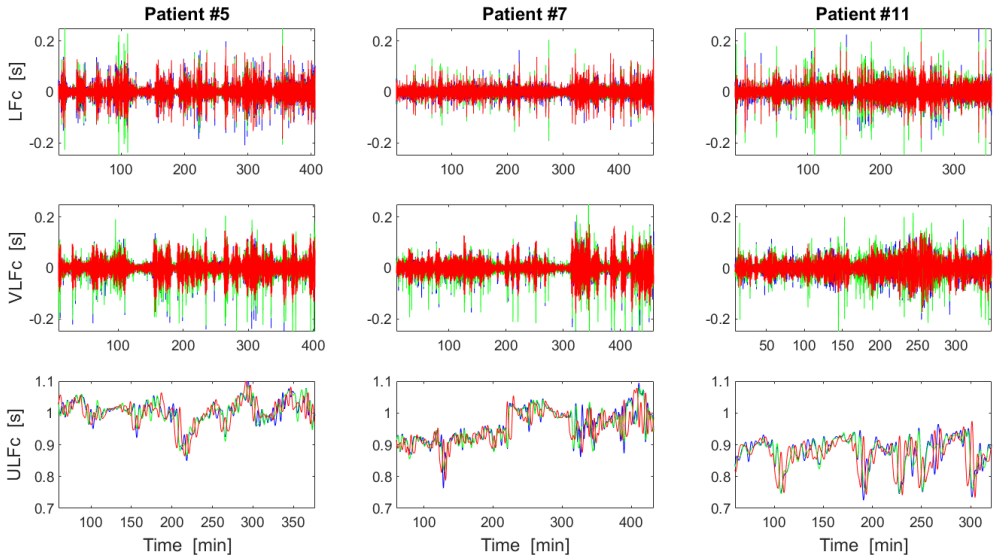

Fig. 3. Low (LFc), very low (VLFc), and ultra-low (ULFc) frequency components of three patients extracted using the three proposed methods: MBF (blue), EMD (green) and STFT (red).

Metrol. Meas. Syst., Vol. 28 (2021), No. 4
DOI: 10.24425/mms.2021.137700

3.3. Amplitude and frequency modulation of components

The instantaneous amplitudes and frequencies of the HFc, LFc, VLFc and ULFc extracted by MBF (blue), EMD (green) and STFT (red, as shown in Figs 2-3 for Patient #7 on the middle panels) were calculated using the HT and presented in Fig. 4. It can be seen that the amplitude modulation assessed by the three methods is consistent (with a slight overestimation in the case of VLFc). However, this does not apply to frequency modulation, where only the results obtained for the ULFc are very similar. In the remaining three cases, the results obtained with EMD are overestimated and the outcomes of STFT underestimated (especially in the case of VLFc) compared to those obtained by the MBF. Nevertheless, the frequency ranges of specific components were always located in the ranges traditionally ascribed to HF, LF, VLF and ULF.

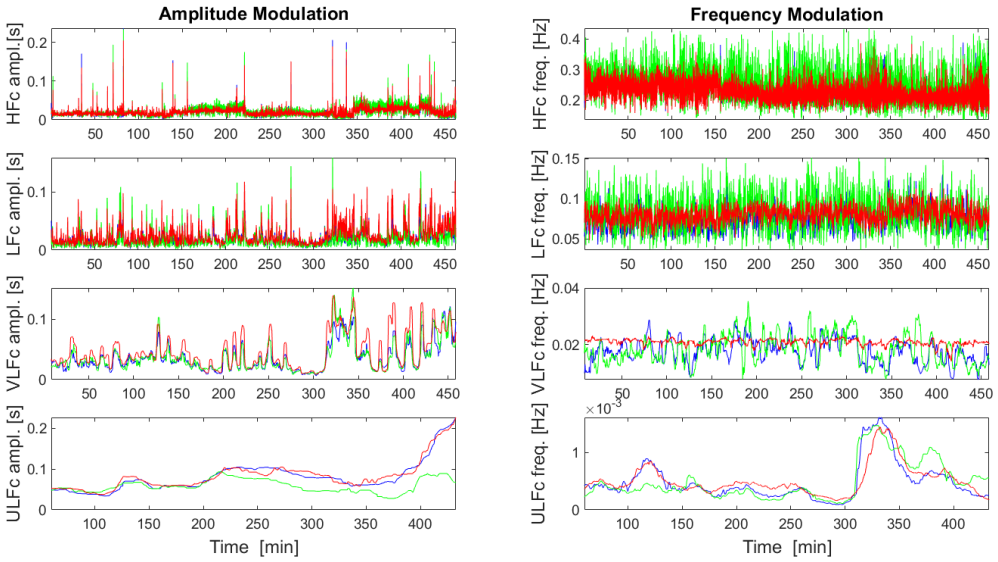

Fig. 4. Instantaneous amplitudes (left panel) and frequencies (right panel) of the HFc, LFc, VLFc and ULFc extracted with MBF (blue), EMD (green) and STFT (red) from the HRV data of Patient #7.

Table 1. Assessed magnitude ranges and frequencies of the AM and FM of the HRV components.

Modulation		**HF**	**LF**	**VLF**	**ULF**
AM	Magnitude range [s]	0.01-0.04	0.01-0.06	0.02-0.08	0.04-0.11
	Modulation frequency [Hz]	0.00105	0.00067	0.00037	0.00022
FM	Magnitude range [Hz]	0.18-0.30	0.06-0.10	0.010-0.025	$0.2\text{-}1.4\times10^{-3}$
	Modulation frequency [Hz]	0.00096	0.00081	0.00045	0.00027

All such results of AM and FM analyses of the frequency components extracted by these three methods from the three patient data series were visually inspected, and the average ranges of magnitudes and frequencies of the modulating signals were then deduced and summarized in Table 1. It can be noticed that the AM amplitude increases as the component frequencies decrease, but the FM amplitude range decreases. Simultaneously, AM and FM frequencies are similar (usually some higher for FM), slightly decreasing as the component frequencies decrease, which is obvious as the absolute ranges of frequency variation also decrease. This information was further used to generate the synthetic HRV waveform (Section 2.8).

3.4. Methods efficiency

The accuracy of the tested methods was analysed on the basis of synthetic HRV, consisting of four nonstationary components, each subjected to AM and FM, and additionally distorted by some random noise. These components together with the known modulation characteristics constitute the ground truth when compared with the extracted signals. In general, all reconstructed signals resembled their ground truth, however, the components obtained with MBF were the most regular.

Table 2. Relative errors (δ) and correlation coefficients (r) of components extracted by the analysed methods.

Component	**Method accuracy**					
	MBF		**EMD**		**STFT**	
	δ [%]	r	δ [%]	r	δ [%]	r
HF	36.0	0.938	58.2	0.856	84.4	0.725
LF	16.7	0.986	41.1	0.915	60.7	0.855
VLF	13.0	0.992	30.3	0.956	124.0	0.292
ULF	0.01	1.000	0.95	0.985	6.34	0.243

The quantitative measures of methods' performance are gathered together in Table 2. Both the relative errors (δ) and correlation coefficients (r) indicate that MBF is the most accurate method for each frequency component. Moreover, the performance indices improve as the component frequencies decrease, except STFT yielding δ = 124% for VLF and very low r for VLF and ULF. This outperformance of MBF is clearly visible in the reconstructed AM and FM traces shown against the real waveforms of the modulating signals in Fig. 5, where only the instantons amplitude of the ULFc has a very approximate trajectory. Another performance indicator is the data processing time, which was completely different for the methods tested. MBF of synthetic HRV_2 (43200 samples) took about 6.7 s (from 10 averaged runs), whereas EMD and STFT: 0.3 and 46.7 s, respectively, and finally HT with smoothing the instantaneous amplitude and frequency about 3.9 s.

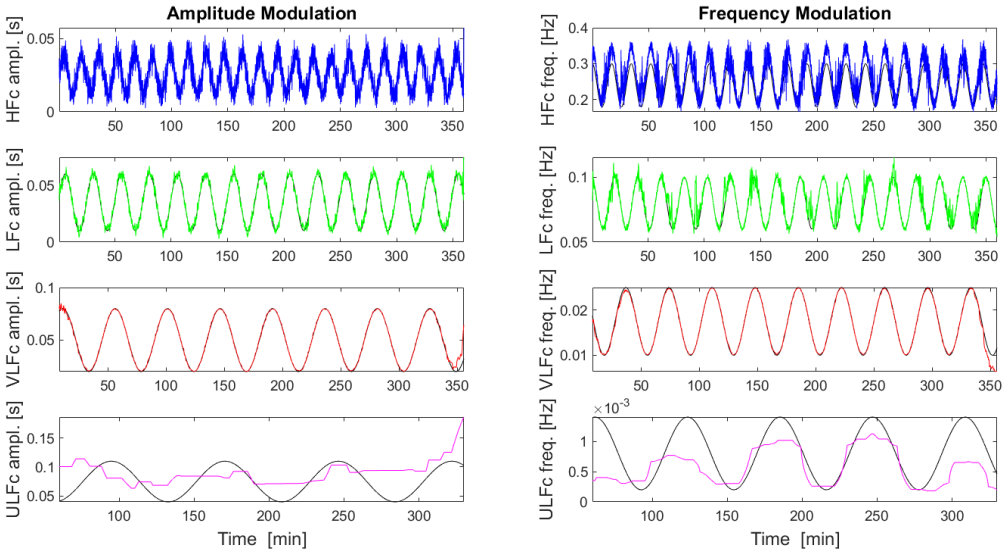

Fig. 5. Instantaneous amplitudes (left panel) and frequencies (right panel) of the HFc, LFc, VLFc and ULFc extracted with MBF from synthetic HRV against their true traces (black).

4. Discussion

The aim of this study was a use-case-based comparison of three methods: MBF, EMD and STFT, used to extract the well-known frequency components (HF, LF, VLF and ULF) from long-term HRV.

The quantitative evaluation of these methods was done on the basis of synthetically generated HRV, where all the details of the nonstationary components subjected to AM and FM were known. This HRV generation routine did not use the frequently applied *integral pulse frequency modulation* (IPFM) model, linking continuous autonomic drive with the discrete and irregular HR. The IPFM model was first introduced by Bayly *et al*. [44] and then modified and used extensively by others [16, 22, 23, 25, 31, 33, 45]. Admittedly, the IPFM model conveys some features of the input drive spectrum to the HRV spectrum, it has been shown that the former spectrum cannot be recovered fully from the latter one [46, 47]. Moreover, it is clear from that model that the instantaneous magnitude of HRV (RR intervals) is roughly inversely proportional to the temporal magnitude of the continuous drive. Summarising, the correct reconstruction of the physiological drives from the extracted components of HRV is a separate inverse problem that has received little attention so far, and is not addressed in this work either. On the other hand, looking at Fig. 1 it is clearly visible that the proposed generation procedure yielded the synthetic signal with spectral properties well matched to the real HRV spectra. Also the preprocessing scheme allowed capturing the true course of cHRV in the regular HRV_2 samples. This means that the used synthetic HRV correctly represented the recovered continuous components. Moreover, it was ensured that changing the regular HRV sampling from 2 to 1 or 4 Hz did not alternate the results of further analyses.

The first of tested methods was MBF. This linear approach has been commonly abandoned since it was realized that HRV is a nonstationary and nonlinear signal [24]. Nevertheless, each of the designed zero-phase FIR filters was matched to a given frequency band which resulted in its specific order (*i.e.* the number of contiguous samples taken into account), lesser for high frequencies and greater for low ones. In other words, the filters acted locally like moving windows, focusing only on the set frequencies and suppressing others. The above explains why this linear tool is still suitable for this particular problem. However, one has to remember that MBF limitation lies in the a priori adopted frequency ranges, which can potentially distort the components when their true spectra are outside these boundaries. On the other hand, at present it seems that the frequency ranges of the autonomous control processes applied are well-established from many other studies, which justifies this approach. Moreover, the components extracted by EMD, which was the only one of the tested methods that did not explicitly assume frequency ranges, are in very good agreement with the results obtained with the MBF, as shown in Figs 2-3 and in [28], which proves that the bands were selected correctly. Ultimately, MBF turned out to be the best method among the tested.

The second method was EMD, and the analyses started with the separation of IMFs from tested HRVs. Ten IMFs were identified in all three patients (16 maximally were allowed) along with residual signals (Fig. 6). This is a larger number than in other studies, where 3-9 IMFs were usually extracted from real data [23, 28, 29]. This difference stems from the much shorter HRV sequences investigated in those works, typically 5 minutes long, so they contained fewer intrinsic modes due to the reduced complexity of such series. Indeed, the EMD of our synthetic 6-hour HRV also returned 10 IMFs, although it consisted of only 4 nonstationary components. The advantage of EMD is that the IMFs do not have predetermined frequencies. Although they were grouped in this work to represent specific frequency components by taking into account the dominant frequencies shown by their histograms, the resulting spectra could still exceed the boundaries and overlap between the components. This may explain why the modulating frequency ranges obtained with EMD were slightly overestimated compared to MBF (Fig. 4).

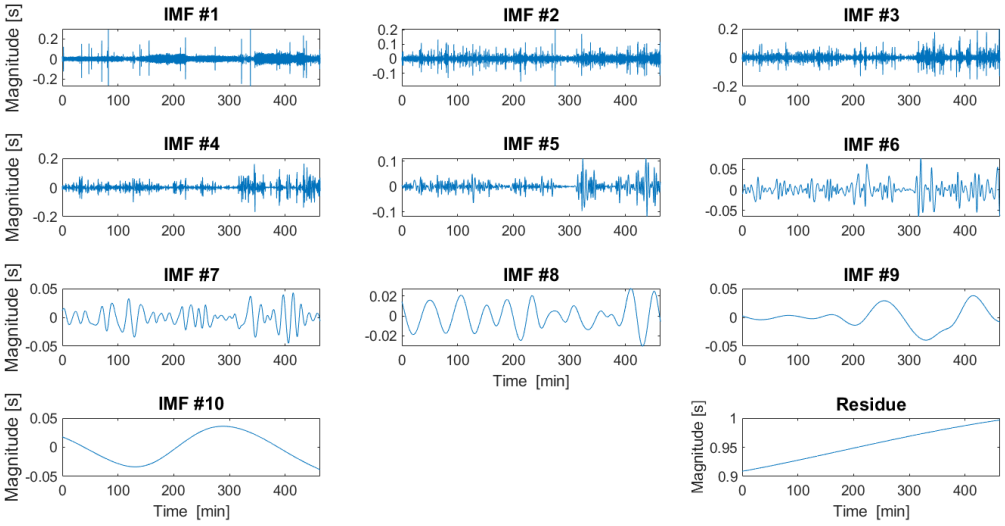

Fig. 6. Intrinsic mode functions (IMFs) and residue resulting from EMD of Patient #7's HRV data.

The third method, STFT, belongs to the most popular in this field, especially due to its suitability for calculating the power spectra of the analysed HRV fragments. Although this approach resulted in components very similar to those from MBF and EMD in terms of their basic shapes and instantaneous amplitudes (Figs 2-3), the instantaneous frequencies assessed for HF, LF and particularly VLF components were more and more suppressed with increasing frequency (right panel). Concurrently, it appears that this reduced FM assessment is compensated for in slightly overestimated AM magnitudes. This may be the effect of double averaging, first used to calculate the instantaneous phases from their temporary spectra (Section 2.5) and then to smooth the modulating frequencies (Section 2.7), so in the future a different approach should be sought to solve this issue. Both the STFT results (as opposed to MBF and EMD) and the averaging effects strongly depend on the sliding window width, which was initially set equal to the longest period characterizing the given frequency band. To investigate the effect of window width, HRV processing was repeated at half width as well as multiplied by 2, 3 and 4, but overall accuracy (in terms of relative standard error) did not improve. Summarising, STFT turned out to be the least accurate approach to extracting physiological components and their properties from HRV.

Despite the observed minor differences in the waveforms extracted by the three methods, the obtained results (especially those presented in Fig. 4) clearly indicate the non-stationarity of the components occurring in HRV, being the subjects to amplitude and frequency modulation. It is also worth noting that AM, similarly recovered from HRV by all the methods (and therefore with greater precision than FM), has a much greater practical significance as it directly represents the magnitude of physiological activity. Summarising, Figs 2-3 as well as Table 1 give a better insight into the overnight impact of the ANS on the HR, at least in terms of the effects that determine the course of HRV, and all the investigated methods followed by the HT are useful in recovering the instantaneous energy of these physiological components.

The analysed methods were quantitatively evaluated in two stages. Firstly, the Resp signals of three patients were compared with the corresponding HF components extracted from HRV, and secondly, the methods performance was assessed on the basis of synthetic data – both in terms of the extracted waveforms similarity and their instantaneous amplitudes and frequencies. Detailed inspection of Fig. 2 shows that Resp and HFc shapes are poorly related to each other, which means that the depth of breathing has no direct impact on HRV in the HF range. However, this conclusion does not apply to frequency coupling between these signals. The

obtained high correlation between both instantaneous phases (r = 0.93 for Patient #7 and 11) is a well-known relationship and proves that MBF combined with the HT is a useful tool for HRV decomposition, at least in the range of HF. The observed correlation can be even greater when the resampling frequency is 4 Hz and the phase shift between the signals can be better fine-tuned [29].

The final comparison between method performances is qualitatively presented in Fig. 5 and quantitatively in Table 2. Admittedly, all the reconstructed components are very similar to the synthetic nonstationary waveforms, nevertheless those extracted with MBF are the smoothest ones and best covering the underlying signals. The effectiveness of MBF, and especially EMD, has also been demonstrated in [28], but in that paper the authors did not provide any details about the filters used. The ultimate outperformance of MBF is presented in Table 2, taking into account all the extracted components as well as both indices – the relative error of component recovering δ and the correlation coefficient r. As recent research on HRV suited to the analysis of nonstationary signals had focused on more modern and advanced methods than MBF, the results obtained here were not obvious. The situation is different with the calculation time, the shortest in the case of EMD (0.3 s), and the longest for STFT (46.7 s). Although EMD is a recurrent routine, it works once on the whole data, while MBF and STFT use the convolution or analysing window, sliding across the data separately for each searched component. Additionally, the instantaneous amplitude and phase are estimated immediately within the applied STFT algorithm. This predestines EMD for online analyses (after appropriate modification).

Looking more closely at the instantaneous amplitudes and frequencies returned by MBF and HT it is clear that these features are most precisely defined in the range of LF and VLF (Fig. 5). Recovered AM and FM from the HFc show random interference that disappears when synthetic undistorted HRV is analysed (checked but not presented here), proving that this effect is due to random perturbations presented in HRV. On the contrary, the distortions in AM and FM of the ULFc remain in this case, showing that they are caused by the processing algorithms themselves, in particular, the known influence of linear filtering on the beginning and end of the processed signal and the applied averaging of the instantaneous amplitudes and frequencies (Section 2.7). Since the instantaneous amplitudes and frequencies resulting from HT had been smoothed, also in this case the effect of the window width was checked. As with the STFT tests, also here the pre-set window width turned out to be the best.

The above results and analyses provided numerous valuable information both in terms of the physiological processes regulating HR and the methods that can be used to study them. Nevertheless, this work has also some limitations. The first crucial one was to investigate the HRV data from only three patients, although many other records exist in the PhysioNet and other public databases. This can be explained by focusing not on the properties of the physiological components themselves, but on methods appropriate for their proper extraction from HRV, and the real data were needed primarily to correctly generate the synthetic waveforms. Another fact worth noting is that the extracted components only represent the effect of ANS activity on HRV and not the underlying physiological drives. As mentioned earlier, recovering the ANS drives from the HRV components is an additional inverse problem that needs to be addressed, but is not covered by this work.

5. Conclusions

This study brings new insights in the area of heart rate variability analysis. It has been shown that the extracted overnight HFc, LFc, VLFc and ULFc are reliable, their nature can therefore be assessed in terms of the instantaneous amplitudes and frequencies. The possibility of

isolating such waveforms is of great importance both in physiology and pathophysiology, as well as in the automation of diagnostics.

The main conclusion is that MBF is more accurate in the overnight HRV frequency analysis than the other two tested methods, *i.e.* EMD and STFT, even though the signal is strongly nonstationary. Moreover, it enables precise recovering the instantaneous amplitudes and frequencies of the HRV components containing HF, LF, VLF and somewhat less accurately ULF, and thus their instantaneous powers and ratios. In summary, the key contribution of this work relies in indicating this best method for extracting HRV components from among the three tested ones.

Future work will focus on a few areas, namely: other up-to-date methods capable of extracting frequency components from nonstationary signals with their reference to MBF, the level of attenuation of ECG/HRV artefacts with these methods, online HRV processing once the basic properties of both its components and the analysing methods are known, as well as the reconstruction of internal ANS drives using the extracted HRV components and the IPFM model.

References

[1] Chyliński, M., & M., Szmajda, M. (2018). Statistical methods for analysing deceleration and acceleration capacity of the heart rate. In Hunek, W., & Paszkiel, S. (Eds.). *Advances in Intelligent Systems and Computing: Vol. 720. Biomedical Engineering and Neuroscience.* (pp. 85–97). Springer. https://doi.org/10.1007/978-3-319-75025-5_9

[2] Sieciński, S., Kostka, P. S., & Tkacz, E. J. (2020). Heart rate variability analysis on electrocardiograms, seismocardiograms and gyrocardiograms on healthy volunteers. *Sensors*, *20*(16), 4522. https://doi.org/10.3390/s20164522

[3] Acharya, R. U., Joseph, P. K., Kannathal, N., Choo, M. L., & Suri, J. S. (2006). Heart rate variability: A review. *Medical and Biological Engineering and Computing*, *44*(12), 1031–1051. https://doi.org/10.1007/s11517-006-0119-0

[4] Shaffer, F., & Ginsberg, J. P. (2017). An overview of heart rate variability metrics and norms. *Frontiers in Public Health*, *5*, 258. https://doi.org/10.3389/fpubh.2017.00258

[5] Goldoozian L. S., Zahedi, E., & Zarzoso, V. (2017). Time-varying assessment of heart rate variability parameters using respiratory information. *Computers in Biology and Medicine*, *89*, 355–367. https://doi.org/10.1016/j.compbiomed.2017.07.022

[6] Boardman, A., Schlindwein, F. S., Rocha, A. P., & Leite, A. (2002). A study on the optimum order of autoregressive models for heart rate variability. *Physiological Measurement, 23*(2), 325–336. https://doi.org/10.1088/0967-3334/23/2/308

[7] Karim, N., Hasan, J. A., & Ali, S. S. (2011). Heart rate variability – A review. *Australian Journal of Basic and Applied Sciences*, *7*(1), 71–77.

[8] Stein, P. K., & Pu, Y. (2012). Heart rate variability, sleep and sleep disorders. *Sleep Medicine Reviews*, *16*(1), 47–66. https://doi.org/10.1016/j.smrv.2011.02.005

[9] Bernardi, L., Valle, F., Coca, M., Calciati, A., & Sleight, P. (1996). Physical activity influences heart rate variability and very-low-frequency components in Holter electrocardiograms. *Cardiovascular Research*, *32*(2), 234–237. https://doi.org/10.1016/0008-6363(96)00081-8

[10] Aoki, K., Stephens, D. P., & Johnson, J. M. (2001). Diurnal variation in cutaneous vasodilator and vasoconstrictor systems during heat stress. *American Journal of Physiology. Regulatory, Integrative and Comparative Physiology*, *281*(2), 591–595. https://doi.org/10.1152/ajpregu.2001.281.2.R591

[11] Fleisher, L. A., Frank, S. M., Sessler, D. I., Cheng, C., Matsukawa, T., & Vannier, C. A. (1996). Thermoregulation and heart rate variability. *Clinical Science*, *90*(2), 97–103. https://doi.org/10.1042/cs0900097

[12] Akselrod. S., Gordon, D., Ubel. F. A., Shannon, D. C., Barger, A. C., & Cohen, R. J. (1981). Power spectrum analysis of heart rate fluctuation: A quantitative probe of beat-to-beat cardiovascular control. *Science*, *213*(4504), 220–222. https://doi.org/10.1126/science.6166045

[13] Porter, G. A., Jr., & Rivkees, S. A. (2001). Ontogeny of humoral heart rate regulation in the embryonic mouse. *American Journal of Physiology. Regulatory, Integrative and Comparative Physiology*, *281*(2), 401–407. https://doi.org/10.1152/ajpregu.2001.281.2.r401

[14] Stampfer, H. G., & Dimmitt, S. B. (2013). Variations in circadian heart rate in psychiatric disorders: Theoretical and practical implications. *ChronoPhysiology and Therapy*, *3*, 41–50. https://doi.org/10.2147/CPT.S43623

[15] Jelinek, H. F., Huang, Z. Q., Khandoker, A. H., Chang, D., & Kiat, H. (2013). Cardiac rehabilitation outcomes following a 6-week program of PCI and CABG patients. *Frontiers in Physiology*, 4, 302. https://doi.org/10.3389/fphys.2013.00302

[16] Li, H., Kwong, S., Yang, L., Huang, D., & Xiao, D. (2011). Hilbert-Huang transform for analysis of heart rate variability in cardiac health. *IEEE/ACM Transactions on Computational Biology and Bioinformatics*, *8*(6), 1557–1567. https://doi.org/10.1109/TCBB.2011.43

[17] Task Force of the European Society of Cardiology the North American Society of Pacing Electrophysiology. (1996). Heart rate variability: Standards of measurement, physiological interpretation, and clinical use. Circulation, 93(5), 1043–1065. https://doi.org/10.1161/01.CIR.93.5.1043

[18] Wen, F., & He, F.-T. (2011). An efficient method of addressing ectopic beats: new insight into data preprocessing of heart rate variability analysis. *Journal of Zhejiang University Science B*, *12*, 976–982. https://doi.org/10.1631/jzus.b1000392

[19] Mendez, M. O., Bianchi, A. M., Matteucci, M., Cerutti, S., & Penzel, T. (2009). Sleep apnea screening by autoregressive models from a single ECG lead. *IEEE Transactions on Biomedical Engineering*, *56*(12), 2838–2850. https://doi.org/10.1109/tbme.2009.2029563

[20] Penzel, T., Kantelhardt, J. W., Grote, L., Peter, J. H., & Bunde, A. (2003). Comparison of detrended fluctuation analysis and spectral analysis for heart rate variability in sleep and sleep apnea. *IEEE Transactions on Biomedical Engineering*, *50*(10), 1143–1151. https://doi.org/10.1109/TBME.2003.817636

[21] Chan, H. L., Chou, W. S., Chen, S. W., Fang, S. C., Liou, C. S., & Hwang, Y. S. (2005). Continuous and online analysis of heart rate variability. *Journal of Medical Engineering and Technology*, *29*(5), 227–234. https://doi.org/10.1080/03091900512331332587

[22] Kudrynski, K., & Strumillo, P. (2015). Real-time estimation of the spectral parameters of heart rate variability. *Biocybernetics and Biomedical Engineering*, *35*(4), 304–316. https://doi.org/10.1016/j.bbe.2015.05.002

[23] Echeverria, J. C., Crowe, J. A., Woolfson, M. S., & Hayes-Gill, B. R. (2001). Application of empirical mode decomposition to heart rate variability analysis. *Medical and Biological Engineering and Computing*, *39*(4), 471–479. https://doi.org/10.1007/bf02345370

[24] Billman, G. E. (2011). Heart rate variability – A historical perspective. *Frontiers in Physiology*, *2*, 86. https://doi.org/10.3389/fphys.2011.00086

[25] Romano, M., Faiella, G., Clemente, F., Iuppariello, L., Bifulco, P., & Cesarelli, M. (2016). Analysis of foetal heart rate variability components by means of empirical mode decomposition. *IFMBE Proceedings*, *57*, 71–74. https://doi.org/10.1007/978-3-319-32703-7_15

[26] Montano, N., Porta, A., Cogliati, C., Costantino, G., Tobaldini, E., Casali, K. R., & Iellamo, F. (2009). Heart rate variability explored in the frequency domain: A tool to investigate the link between heart and behavior. *Neuroscience and Biobehavioral Reviews*, *33*(2), 71–80. https://doi.org/10.1016/j.neubiorev.2008.07.006

[27] Huang, N. E., Shen, Z., Long, S. R., Wu, M. C., Shih, H. H., Zheng, Q., Yen, N.-C., Tung, C. C., & Liu, H. H. (1998). The empirical mode decomposition and the Hilbert spectrum for nonlinear and non-stationary time series analysis. *Proceedings of The Royal Society of London A*, *454*(1971), 903–995. https://doi.org/10.1098/rspa.1998.0193

[28] Chen, M., He, A., Feng, K., Liu, G., & Wang, Q. (2019). Empirical mode decomposition as a novel approach to study heart rate variability in congestive heart failure assessment. *Entropy*, *21*(12), 1169. https://doi.org/10.3390/e21121169

[29] Balocchi, R., Menicucci, D., Santarcangelo, E., Sebastiani, L., Gemignani, A., Ghelarducci, B., & Varanini, M. (2004). Deriving the respiratory sinus arrhythmia from the heartbeat time series using empirical mode decomposition. *Chaos, Solitons & Fractals*, *20*(1), 171–177. https://doi.org/10.1016/S0960-0779(03)00441-7

[30] Ortiz, M. R., Bojorges, E. R., Aguilar, S. D., Echeverria, J. C., Gonzalez-Camarena, R., Carrasco, S., Gaitan, M. J., & Martinez, A. (2005). Analysis of high frequency fetal heart rate variability using empirical mode decomposition. *Computers in Cardiology*, France, 675–678. https://doi.org/10.1109/CIC.2005.1588192

[31] Helong, L., Yang, L., & Daren, H. (2008). Application of Hilbert-Huang transform to heart rate variability analysis. *2nd International Conference on Bioinformatics and Biomedical Engineering*, China, 648–651. https://doi.org/10.1109/ICBBE.2008.158

[32] Neto, E. P. S., Custaud, M. A., Cejka, J. C., Abry, P., Frutoso, J., Gharib, C., & Flandrin, P. (2004). Assessment of cardiovascular autonomic control by the empirical mode decomposition. *Methods of Information in Medicine*, *43*(1), 60–65. https://doi.org/10.1055/s-0038-1633836

[33] Ihlen, E. A. F. (2009). A comparison of two Hilbert spectral analyses of heart rate variability. *Medical & Biological Engineering & Computing*, *47*(10), 1035–1044. https://doi.org/10.1007/s11517-009-0500-x

[34] Eleuteri, A., Fisher, A. C., Groves, D., & Dewhurst, C. J. (2012). An efficient time-varying filter for detrending and bandwidth limiting the heart rate variability tachogram without resampling: MATLAB open-source code and internet web-based implementation. *Computational and Mathematical Methods in Medicine*, 2012, Article 578785. https://doi.org/10.1155/2012/578785

[35] Fisher, A. C., Eleuteri, A., Groves, D., & Dewhurst, C. J. (2012). The Ornstein–Uhlenbeck third-order Gaussian process (OUGP) applied directly to the un-resampled heart rate variability (HRV) tachogram for detrending and low-pass filtering. *Medical and Biological Engineering and Computing*, *50*(7), 737–742. https://doi.org/10.1007/s11517-012-0928-2

[36] Varanini, M., Macerata, A., Emdin, M., & Marchesi, C. (1994). Non linear filtering for the estimation of the respiratory component in heart rate. *Computers in Cardiology*, USA, 565–568. https://doi.org/10.1109/CIC.1994.470129

[37] Estévez, M., Machado, C., Leisman, G., Estévez-Hernández, T., Arias-Morales, A., Machado, A., & Montes-Brown, J. (2016). Spectral analysis of heart rate variability. *International Journal on Disability and Human Development*, *15*(1), 5–17. https://doi.org/10.1515/ijdhd-2014-0025

[38] McCraty, R., & Shaffer, F. (2015). Heart rate variability: New perspectives on physiological mechanisms, assessment of self-regulatory capacity, and health risk. *Global Advances in Health and Medicine*, *4*(1), 46–61. https://doi.org/10.7453/gahmj.2014.073

[39] Nunan, D., Sandercock, G. R. H., & Brodie, D. A. (2010). A quantitative systematic review of normal values for short-term heart rate variability in healthy adults. Pacing and Clinical Electrophysiology, 33(11), 1407–1417. https://doi.org/10.1111/j.1540-8159.2010.02841.x

[40] Goldberger, A., Amaral, L., Glass, L., Hausdorff, J., Ivanov, P. C., Mark, R., Mietus, J. E., Moody, G. B., Peng, C. K., & Stanley, H. E. (2000). PhysioBank, PhysioToolkit, and PhysioNet: Components of a new research resource for complex physiologic signals. *Circulation*, *101*(23), 215–220. https://doi.org/10.1161/01.cir.101.23.e215

[41] Terzano, M. G., Parrino, L., Sherieri, A., Chervin, R., Chokroverty, S., Guilleminault, C., Hirshkowitz, M., Mahowald, M., Moldofsky, H., Rosa, A., Thomas, R., & Walters, A. (2001). Atlas, rules, and recording techniques for the scoring of cyclic alternating pattern (CAP) in human sleep. Sleep Medicine, 2(6), 537–553. https://doi.org/10.1016/s1389-9457(01)00149-6

[42] Jun, S., Szmajda, M., Khoma, V., Khoma, Y., Sabodashko, D., Kochan, O., & Wang, J. (2020). Comparison of methods for correcting outliers in ECG-based biometric identification. *Metrology and Measurement Systems*, *27*(3), 387–398. https://doi.org/10.24425/mms.2020.132784

[43] Hsu, M.-K., Sheu, J.-C., & Hsue, C. (2011). Overcoming the negative frequencies: instantaneous frequency and amplitude estimation using osculating circle method. *Journal of Marine Science and Technology*, *19*(5), 514–521. https://doi.org/10.6119/JMST.201110_19(5).0007

[44] Bayly E. J. (1968). Spectral analysis of pulse frequency modulation in the nervous systems. *IEEE Transactions on Biomedical Engineering*, *15*(4), 257–265. https://doi.org/10.1109/TBME.1968.4502576

[45] Mateo, J., & Laguna, P. (1996). New heart rate variability time-domain signal construction from the beat occurrence time and the IPFM model. *Computers in Cardiology*, USA, 185–188. https://doi.org/10.1109/CIC.1996.542504

[46] de Boer, R. W., Karemaker, J. M., & Strackee, J. (1985). Spectrum of a series of point events, generated by the integral pulse frequency modulation model. *Medical and Biological Engineering and Computing*, *23*(2), 138–142. https://doi.org/10.1007/BF02456750

[47] Nakao, M., Norimatsu, M., Mizutani, Y., & Yamamoto, M. (1997). Spectral distortion properties of the integral pulse frequency modulation model. *IEEE Transactions on Biomedical Engineering*, *44*(5), 419–426. https://doi.org/10.1109/10.568918